Proceedings of the Pakistan Academy of Sciences: A Physical and Computational Sciences 61(1): 61-69 (2024)

ISSN (Print): 2518-4245; ISSN (Online): 2518-4253
https://doi.org/10.53560/PPASA(61-1)793

Pakistan Academy of Sciences

Research Article

Experimental Implementation and Analysis of Microwave Power Dividers and Directional Couplers

Imad Ali[1*], and Nasir Saleem[2]

[1]Department of Computer Science, University of Swat, Pakistan
[2]Department of Electrical Engineering, Faculty of Engineering and Technology, Gomal University, Dera Ismail Khan, Pakistan

Abstract: In radio technology, directional couplers and power dividers play a vital role. These devices have well-established theories; however, their performance is not studied under diverse input voltages (and frequencies). This article analyzes the aforementioned devices via extensive laboratory hardware experiments under various input voltages and frequency band settings. The splited power is measured and examined at detectors and ports, while additional parameters, including Insertion Loss and Directivity, are used. The experimental analysis of microwave devices is examined for the power split over a band of frequencies. Our experimental results over a frequency band of 2.0 to 3.0 GHz (with a step size of 0.1 GHz) show that transmitted power at low frequencies is equal and is slightly affected at higher frequencies while the power splitting characteristic over a band of frequencies matches their theories.

Keywords: Microwave Devices, Power Dividers, Directional Couplers, Insertion Loss, Directivity.

1. INTRODUCTION

In radio technology, directional couplers (DCs) and power dividers (PDs) play a vital role [1]. A certain amount of the electromagnetic (EM) power in the transmission line is linked via these devices that can be used in other circuits [2]. The EM power can only be coupled to an isolated port [3]. A DC is used when there is a desire to equalize power. It consists of two linked transmission lines designed so that EM power in one line in a given direction is linked to the other line, propagating only in one direction but not in another, which is a vital characteristic of the DCs [4]. The description of coupling, coupling properties, and directivity can be explained with the help of Figure 1. Figure 1(A) shows the EM power incidents (carried by electromagnetic waves) at the port 1, and power appears at the coupled port, port 3. No decoupled power appears at port 4. Likewise, when the EM power incidents at the port 2, the power appears at the coupled port, port 4, and no decoupled power appears at port 3, as shown in Figure 1(B). Therefore, such coupling is directional. The coupling coefficient of the DC can be defined as:

$$\kappa = \frac{\text{Port}_3}{\text{Port}_1} \tag{1}$$

Assuming all ports are matched, the coupling is usually expressed in dB and is given as:

$$C_{\text{OUPLING}} = 10\log_{10}\left(\frac{P_3}{P_1}\right) = 20\log\left(\frac{P_3}{P_1}\right) \tag{2}$$

Directivity is used as a measure of coupling properties and can be defined as the ratio of the power to a decoupled port to the power at the coupled port, given by the formula:

$$D_{\text{IRECTIVITY}} = 10\log_{10}\left(\frac{P_4}{P_3}\right) = 20\log\left(\frac{P_4}{P_3}\right) \tag{3}$$

The insertion loss can be calculated from the following formula:

$$I_{\text{nsertion}}L_{\text{oss}} = 20\log_{10}\left(\frac{P_2}{P_1}\right) \tag{4}$$

On the other hand, power dividers (PD) divide

Received: October 2022; Revised: November 2023; Accepted: March 2024
*Corresponding Author: Imad Ali <imadali@uswat.edu.pk>

the input EM signals into two in-phase EM signals [5]. The PDs can also be used to combine power. The common port is the output port, whereas the other two ports are exploited as the input ports. Necessary design provisions for the PDs contain insertion loss, amplitude, and phase balance between arms and return losses. Intended for the power combining of uncorrelated EM signals, the most vital design specification is the isolation, that is, the insertion loss from one equal power port to another. Figure 2 shows the Wilkinson PD with two parallel uncoupled quarter-wavelength transmission lines (λ/4 length). The input is provided to two corresponding lines, and the outputs are ended with matching impedance. To avoid coupling, both the lines must be kept spaced; and must get back together at outputs. The impedances at all ports must be the same as the microwave system's characteristic impedance (normally,70 Ω) [6].

Similarly, the rat-race hybrid ring coupler (RHRC) [7], is a four-port device with a transmission line of the mean circumference of 3/4λg with four pots spaced, as shown in Figure 3. The EM power supplied at one port to the RHRC splits equally to the two head-to-head ports, and no EM power appears at the remaining port. The characteristic impedance of the ring line is matched when it is equal to $\sqrt{2}Z_O$. Thus, for a 50 Ω system, $\sqrt{2}Z_O$ = 70.7 Ω. The operation of the RHRC is illustrated in Figure 3**,** where the input EM power at ports 1 appears at ports 2 and 4. Ignoring the power losses, the output EM powers are 3dB down (i.e., half-power) compared to the incident EM power, but these are in phase by 180 degrees due to a half-wavelength difference in their parts through the ring [8]. No power appears at port 3 since waves following path 1 Ø 2 Ø 3 travel $1/2\lambda_g$. Whilst those traveling 1 Ø 4 Ø 3 cover λ_g and hence the path difference is $1/2\lambda_g$. The two components are thus in anti-phase and cancel.

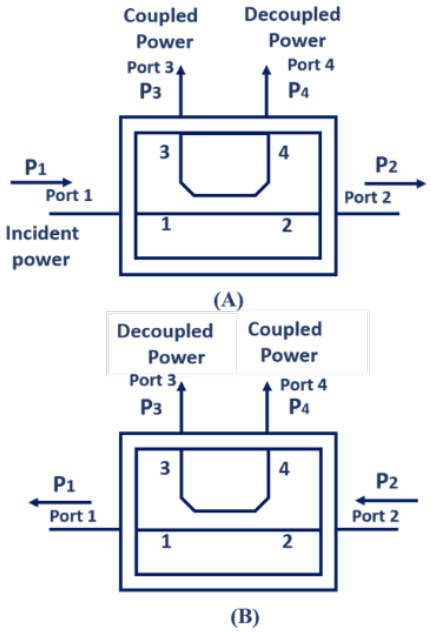

Fig. 1. Schematic diagram of directional coupler transmission properties: (A) Port 1 incident power, (B) Port 2 incident power.

In the past, microwave components like equal PDs, Quadrature Hybrid Couplers, and Rat Race Hybrid Ring couplers were designed for their isolation and matching properties but hinting at the potential for high symmetry and bandwidth enhancement [9]. Studies on Wilkinson power dividers demonstrated their capacity to split power into equiphase segments with isolation between output ports, achieving -27dB isolation and favorable VSWR values [10]. A proposed 90˚ hybrid coupler showcased a compact design with an 18.2% bandwidth enhancement [11]. An Evolutionary Algorithm demonstrated competence in a slot-coupled 3-dB hybrid coupler [12]. Exploration of stub-loaded transmission lines for Wilkinson

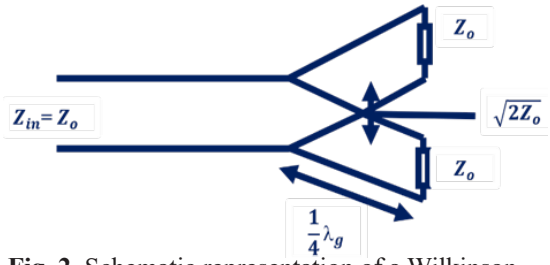

Fig. 2. Schematic representation of a Wilkinson Power Divider.

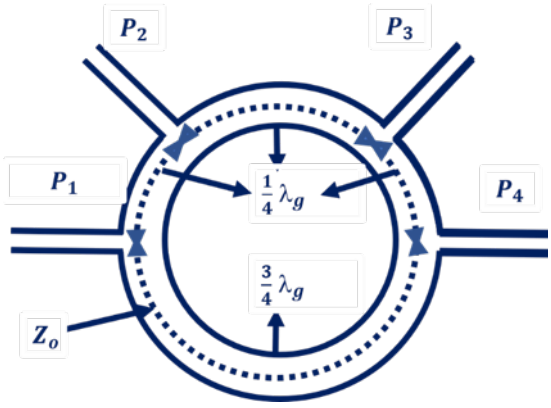

Fig. 3. Illustration depicting a Rat-Race Hybrid Ring Coupler.

PDs demonstrated adaptability for unequal power divisions [13]. Microstrip designs achieved size reduction, and harmonic suppression, maintaining traditional PD features [14]. Capacitive loading in planar Wilkinson PDs improved efficiency, resulting in miniaturized dividers with superior performance [15]. Various methods for 6-dB coupler realization, including rat-race and ring couplers, were explored, acknowledging limitations such as low isolation and specific frequency range constraints [16].

These devices have well-established theories; however, their performance is not studied under diverse input voltages (and frequencies). This article analyzes the aforementioned devices via extensive laboratory hardware experiments under various input voltages and frequency band settings. The primary contribution of this paper lies in the rigorous experimental analysis of microwave power dividers and directional couplers under conditions not extensively explored in existing literature. While prior studies have established the theoretical foundations of these devices, our research provides a practical examination of their performance, particularly focusing on power-splitting characteristics over a broad spectrum of frequencies. In contrast to earlier works that may have limited their investigations to specific frequency ranges or neglected the impact of varying input voltages, our experiments reveal nuanced insights. We address the gap in the literature by demonstrating that transmitted power is only slightly affected at higher frequencies, and the power splitting characteristic holds true across diverse frequency bands.

The present research aimed to address and overcome some of the limitations identified in the previous works. The proposed study conducts extensive laboratory experiments under various input voltages and frequency bands, providing a comprehensive analysis of microwave power dividers and directional couplers. By exploring a broader range of operating conditions, the present research seeks to enhance the understanding of these devices and uncover potential performance variations not covered in previous studies. Moreover, the proposed work delves into the experimental analysis of power splitting characteristics over a band of frequencies, evaluating parameters such as Insertion Loss and Directivity. It may allow to assess the behavior of the devices beyond their specified frequency bands, providing valuable insights into their practical applicability. The experimental results showed that transmitted power is slightly affected at higher frequencies while the power splitting characteristic over a band of frequencies matches their theories.

2. EXPERIMENTS DESIGN

This section outlines various experiments conducted to assess directional couplers (DCs) and power dividers (PDs) across a range of frequencies and VCO voltages. The experiment includes: (a) investigating and measuring directional properties and determining the Coupling, Directivity, and Insertion Loss of DCs, (b) investigating the power division characteristics over a band of frequencies, and (c) investigating how power splits in the branch line coupler. The details about the hardware implementation used to perform the experiments mentioned above are given in Table 1.

For power splitting**,** microwave power dividers and directional couplers are designed to split the input power into multiple outputs. The coupling properties are fundamental to their operation. The coupling coefficient, as defined in Equation (1) in the paper, is a crucial parameter. It quantifies the ability of the device to split power between different ports. The paper conducts extensive laboratory hardware experiments under various input voltages and frequency band settings. By measuring the power at different ports and detectors, the experimental results provide insights into the actual power-splitting characteristics of the devices. These results are crucial for validating the theoretical expectations and understanding how the devices perform in practical scenarios.

The impact of higher frequencies on transmitted power is considered in the paper, where transmitted power may vary with increasing frequencies. Through the hardware experiments, the paper analyzes the stability of transmitted power at higher frequencies. By varying the input frequency and measuring the transmitted power, the experimental results reveal the device's performance under different frequency bands. This experimental evidence is essential for understanding how the devices handle transmitted power across a spectrum of frequencies.

Table 1. Hardware description used in experiments.

S. No.	Module	Description
1	Microstrip Base	Voltage Controlled Oscillator: Tunable over range 2GHz to 4GHz, RF Detector: Input +5 dBm and Power Range: -45dBm ~ -5dBm
2	Directional Coupler	Microstrip components with Directional Transmission, properties used to measure Power Reflection Coefficient, Return loss.
3	3dB Attenuator	Microstrip attenuator producing a transmission loss of 3 dB
4	Hybrid Coupler	Microstrip component designed to couple incident power at one port equally to two other ports but provide isolation between the incident and a fourth port.
5	Wilkinson Power Divider	Microstrip component designed to split incident microwave power equally to its two output ports.
6	Rat race Hybrid Coupler	Microstrip component designed to couple incident power at one port equally to two other ports but provide isolation between the incident and a fourth port.
7	Three Port Circulator	Ferrite circulator mounted in Microstrip used for its non-reciprocal transmission properties widely used as an isolator, diplexer, and channel separator

Directivity and Insertion loss are critical parameters in microwave devices. These parameters have been defined in Equations (3) and (4), respectively. Insertion loss quantifies the power loss between the input and output ports, while directivity measures the ability of the device to couple power to a specific port while minimizing power to other ports. The experimental analysis in the paper includes measurements of insertion loss and directivity. These measurements provide practical insights into how the devices perform in terms of power loss and coupling efficiency. The experimental results are compared with the theoretical expectations, enhancing the understanding of the devices' real-world behavior.

2.1. Directional Properties, Directivity, and Insertion Loss

In the first experiment, the results are obtained to show coupling, directivity, and insertion loss of the DC over the range of 2.0 GHz to 3GHz band. Figures 4 and 5 show the experimental setup. P1 is measured using the circuit in Figure 5, where a 3-port circulator is used as an isolator for the voltage-controlled oscillator (VCO) microwave source with low transmission from port1 to port2. The coupled power P3 is measured. Ports 2 and port 4 are matched with a characteristic impedance. The crystal detector is used for a suitable match at port 3. The Power P4 to the decoupled port is measured, whereas port 2 and port 3 are terminated with a 50Ω matched load. Finally, transmission power P2 is measured, whereas port 3 and port 4 are terminated with a 50Ω matched load. The use of a 3-port circulator as an isolator for the VCO helped reduce transmission losses from port 1 to port 2. The use of a 3-port circulator as an isolator for the VCO helped reduce transmission losses from port 1 to port 2. The transmission coefficient (S_{21}) can be expressed as:

$$S_{21} = e^{-j\beta l} \tag{5}$$

where β is the propagation constant and l is the length of the transmission line. Additionally, ports 2 and 4 were matched to the characteristic impedance (Z_0) to optimize energy transfer. The reflection coefficient (ΓΓ) at a matched load can be given by:

$$\Gamma = \frac{Z_L+Z_0}{Z_L-Z_0} \tag{6}$$

where Z_L is the load impedance.
The crystal detector at port 3 ensured a suitable match, contributing to minimizing losses. The power transfer coefficient (T) for a matched load can be expressed as:

$$T = 1 - |\Gamma|^2 \tag{7}$$

Terminating ports 2 and 3 with a 50Ω matched load further assisted in containing energy losses, ensuring that the incident and transmitted powers are efficiently transferred.

2.2 Power Splitting Characteristics over Band of Frequencies

A critical characteristic that determines the superiority of a microwave PD is the degree to which the input EM power is divided [9]. Thus,

Fig. 4. Experimental layout with hardware connection in the laboratory.

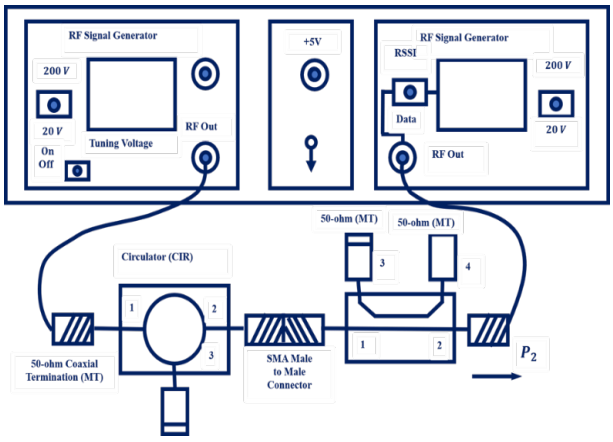

Fig. 5. Schematic detailing the hardware connections for an experimental setup in the laboratory.

when lines are matched, the EM power splits equally between the two output lines. The input VSWR and isolation between the output lines are also important. We have investigated the splitting potential of the Wilkinson PD and the RHRC. The equipment setup is shown in Figures 4 and 5**,** with the third PD port terminated with a 50Ω load to match this port. Directional Couplers (DCs) and Power Dividers (PDs) operate within the microwave range (2.0 GHz to 3 GHz) and undergo analysis with a step size of 0.1 GHz. Using the voltage frequency calibration data supplied, set the VCO to 2.0 GHz. Energy losses in the directional coupler (DC) were minimized using a 3-port circulator as an isolator, matched ports, and 50Ω load termination and in assessing power splitting characteristics over a frequency band, energy loss mitigation involved VCO calibration and careful port termination with matched loads for optimized energy transfer. The power P2 emerging from port 2 at the input RF signal generator is measured. Repeated the power measurement at 0.1GHz intervals through the band up to 3 GHz and recorded the results. A 50 Ω termination is connected to port P2 and connected port P3 to the RF input of the signal detector, so Power P3 at port 3 can be measured with port 2 matched. The power emerging at port 3 is measured and recorded the results from 2 GHz to 3GHz.

3. RESULTS AND DISCUSSION

Tables 2-4 present a detailed analysis of detector voltage, incident and transmitted power, coupled and decoupled powers, directivity, and insertion loss. The following elaboration provides a nuanced interpretation of the presented results.

3.1. Coupled and Decoupled Power Analysis

Table 2 provides a comprehensive analysis of coupled and decoupled power for different frequencies (GHz) and corresponding VCO voltages.

The decoupled power (P4) represents the power that is isolated from the system, while the coupled power (P3) indicates the power that is influenced by the system. As the frequency increases, the decoupled power initially rises but eventually becomes negative, signifying a shift towards the system's influence. The coupled power demonstrates a consistent decrease, indicating the diminishing impact of the system. This table serves as a valuable reference for understanding the intricate relationship between frequency, VCO voltage, and the distribution of coupled and decoupled powers in the presented analysis.

Table 2. Coupled and decoupled power.

Fr (GHz)	VCO (Volts)	Decoupled Power P4 (dBm)	Coupled Power P3 (dBm)
2.0	2.01	2.082911	0.069211
2.1	2.70	1.783967	-0.11366
2.2	3.30	1.554624	-0.28249
2.3	4.10	1.378552	-0.3365
2.4	4.90	1.206401	-0.29147
2.5	5.70	0.788282	-0.55594
2.6	6.60	0.440315	-0.71481
2.7	7.41	-0.03481	-0.96354
2.8	8.31	-0.05227	-0.73369
2.9	9.30	-2.32677	-2.90174
3.0	10.0	-4.49507	-4.64205

Table 3. Incident power and transmitted power analysis after passing three detectors.

Fr (GHz)	VCO (Volts)	Incident Power P1 (dBm)	Detector Volts V1	Detector Volts V2	Detector Volts V3	Detector Volts V4	Transmitted Power P2 (dBm)
2.0	2.01	4.65	1.71	1.70	1.00	1.27	4.62
2.1	2.70	4.45	1.67	1.67	0.98	1.22	4.45
2.2	3.30	4.30	1.64	1.64	0.96	1.19	4.33
2.3	4.10	4.30	1.64	1.63	0.96	1.17	4.29
2.4	4.90	4.19	1.62	1.62	0.96	1.14	4.20
2.5	5.70	4.08	1.60	1.59	0.93	1.09	3.94
2.6	6.60	3.99	1.58	1.58	0.92	1.05	3.81
2.7	7.41	4.16	1.61	1.60	0.89	0.99	3.98
2.8	8.31	3.85	1.55	1.55	0.91	0.99	3.75
2.9	9.30	3.37	1.47	1.44	0.71	0.76	3.19
3.0	10.0	1.99	1.23	1.25	0.58	0.59	1.88

3.2. Incident Power and Transmitted Power Analysis

Table 3 delves into incident power, detector voltages, and transmitted power after passing three detectors. The results showcase a consistent trend where incident power decreases with increasing VCO voltage. Simultaneously, the transmitted power demonstrates a similar pattern. This behavior highlights the impact of VCO voltage on both incident and transmitted powers, providing valuable insights for optimizing power transmission efficiency [9].

3.3. Directivity and Insertion Loss Analysis

Table 4 focuses on directivity and insertion loss analysis. The coupling, directivity, and insertion loss are computed from hardware readings, revealing intriguing patterns. The directivity remains relatively stable across frequencies, indicating consistent isolation between ports. Additionally, the insertion loss, though minimal, displays slight variations. This emphasizes the need for careful consideration of insertion loss in practical applications, especially at higher frequencies.

3.4. Power Tracking Analysis of Wilkinson Power Divider

The power tracking analysis results, presented in Table 5 offers a comprehensive overview of power distribution across different ports of the Wilkinson Power Divider (PD). The results suggest an effective power division at lower frequencies, with a slight deviation at higher frequencies. This behavior is mirrored in the detected voltages at these ports, affirming the splitting capabilities of the Wilkinson PD.

3.5. Rat-Race Hybrid Ring Coupler Investigation

Table 6 provides the details of the investigation of the Rat-Race Hybrid Ring Coupler (RHRC). The powers at ports 1 and 3 exhibit similarity at lower frequencies, with a gradual difference emerging at higher frequencies. This trend aligns with the detected voltages at these ports, emphasizing the frequency-dependent behavior of the RHRC.

Table 4. Directivity and insertion loss analysis.

Fr (GHz)	Coupling (P1-P3) dB	Directivity (P4-P3) dB	Insertion Loss (P1-P2) dB
2.0	4.59	2.01	0.035
2.1	4.57	1.89	0.005
2.2	4.62	1.83	0.005
2.3	4.63	1.71	0.010
2.4	4.48	1.49	-0.010
2.5	4.64	1.34	0.043
2.6	4.70	1.15	-0.016
2.7	5.13	0.92	0.081
2.8	4.59	0.68	0.000
2.9	6.27	0.57	0.184
3.0	6.44	0.14	-0.181

Table 5. Wilkinson Power Divider power tracking analysis.

Fr (GHz)	VCO (Volts)	Detector Volts V2	Power at P2 (dBm)	Detector Volts V3	Power at P3 (dBm)
2.0	2.0	1.67	4.45	1.67	4.45
2.1	2.5	1.64	4.34	1.64	4.33
2.2	3.5	1.62	4.21	1.62	4.21
2.3	4.5	1.60	4.08	1.60	4.09
2.4	5.5	1.55	3.85	1.56	3.86
2.5	6.5	1.53	3.73	1.53	3.69
2.6	7.5	1.46	3.34	1.46	3.31
2.7	8.5	1.31	2.37	1.31	2.40
2.8	9.5	1.15	1.23	1.15	1.26
2.9	10.5	0.95	-0.39	0.95	-0.44
3.0	11.5	1.07	0.62	1.08	0.69

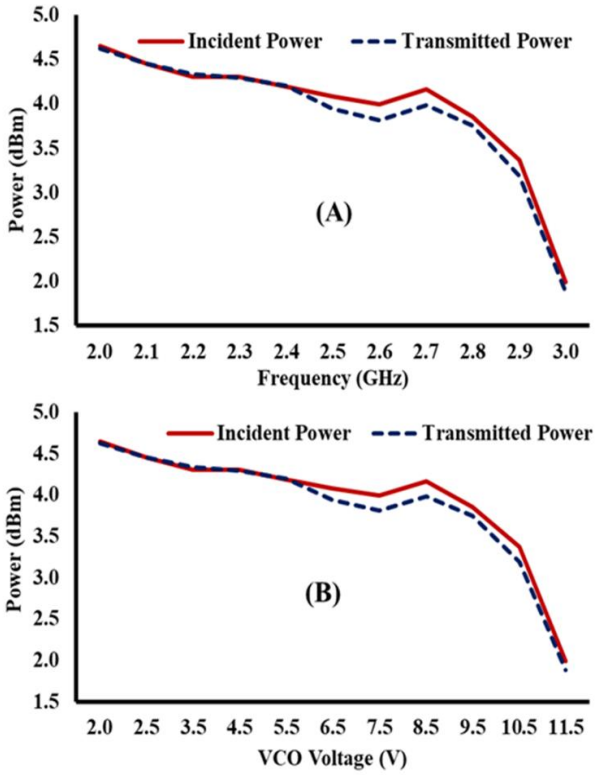

Fig. 6. Incident and transmitted power analysis of frequency band (A) with respect to the input voltage for a Voltage-Controlled Oscillator (B).

3.6. Power Analysis Regarding VCO Input Voltage and Frequency Band

The analysis of incident and transmitted power for frequency band is illustrated in Figure 6 (A), while the same analysis concerning input voltage in a VCO is shown in Figure 6(B). Figure 6 provides a visual representation of power analysis concerning VCO input voltage and the frequency band. The power tracking trends affirm the consistent behavior observed in the tables, further validating the stability and reliability of the proposed devices within their designed frequency bands.

3.7. Theoretical Validation and Frequency-Dependent Losses

The results obtained in these experiments align with theoretical expectations within the designed frequency bands [9]. The observed losses at higher frequencies underscore the importance of assessing device performance in practical settings, where deviations from designed frequency bands can impact overall efficiency. This analysis provides a crucial understanding of the practical implications of the proposed devices, informing future design considerations and applications.

The results obtained from the present experiments match with the theories at the designed frequency bands [9]. The reason for the slight difference at higher frequencies is that these devices are fabricated and designed for particular frequencies (or certain bands). When they operate in the designed frequency bands, their losses are minimal. However, their losses increase when they are used at different frequency bands. Thus, it is crucial to find the losses associated with it in practical settings, as analyzed in this article. In summary, the comprehensive results and their detailed interpretation enhance our understanding of the proposed devices' performance characteristics, offering valuable insights for both theoretical advancements and practical applications.

Table 6. Rat-Race Hybrid Ring coupler investigation.

VCO (Volts)	Detector Volts V1	Power at P1 (dBm)	Detector Volts V2	Power at P2 (dBm)	Detector Volts V3	Power at P3 (dBm)
2.0	1.69	4.58	1.66	4.43	1.66	4.41
2.5	1.66	4.44	1.64	4.34	1.63	4.28
3.5	1.64	4.31	1.62	4.21	1.62	4.21
4.5	1.62	4.19	1.59	4.05	1.59	4.07
5.5	1.58	4.00	1.55	3.84	1.56	3.87
6.5	1.56	3.91	1.52	3.65	1.54	3.78
7.5	1.53	3.74	1.38	2.80	1.46	3.28
8.5	1.40	2.97	1.35	2.63	1.30	2.30
9.5	1.25	1.97	1.42	3.08	0.99	-0.00
10.5	1.11	0.96	1.13	1.06	0.67	-3.36
11.5	1.25	1.93	1.20	1.61	0.81	-1.79

4. SUMMARY AND CONCLUSIONS

This article presents an intense analysis of microwave PDs and DCs regarding the splited power, detector voltage, and frequency bands. The experiments and analysis are performed by hardware implementations. Wilkinson PDs, DCs, and Rat-RHRC are used in experiments. During the experiments, PDs and RHRCs are analyzed for different input VCO voltages and bands of frequencies. The split power is then measured and examined at detectors and ports. In the case of the DCs, additional parameters, including Insertion Loss and Directivity. The experimental analysis of microwave devices has shown how power splits in microstrip systems. After practical experiments, it is analyzed that the transmitted power is somehow affected at higher frequencies. Moreover, the PDs showed equal power splitting at different ports. The splitting characteristics over a band of frequencies are observed according to theoretical discussions.

5. CONFLICT OF INTEREST

The authors declare no conflict of interest.

6. REFERENCES

1. X. Guan, H. Wu, Y. Shi, L. Wosinski, and D. Dai. Ultracompact and broadband polarization beam splitter utilizing the evanescent coupling between a hybrid plasmonic waveguide and a silicon nanowire. *Optics Letters* 38(16): 3005-3008 (2013).
2. A. Collado, and A. Georgiadis. Conformal hybrid solar and electromagnetic (EM) energy harvesting rectenna. *IEEE Transactions on Circuits and Systems I: Regular Papers* 60(8): 2225-2234 (2013).
3. X. Hu, and F. Xu. A six-port network based on substrate substrate-integrated waveguide coupler with metal strips. *IET Microwaves, Antennas & Propagation* 16(1): 18-28 (2022).
4. D.A. Letavin, Y.E. Mitelman, and V.A. Chechetkin. Compact microstrip branch-line coupler with unequal power division. *11th IEEE European Conference on Antennas and Propagation (EUCAP)* 1162-1165 (2017).
5. A.I. Omi, M.H. Maktoomi, M.A. Maktoomi, and P.K. Sekhar. Miniaturized Wideband Three-Way Power Dividers with Arbitrary Band Ratio Using a New Analytical Design Technique. *IEEE Access* 11: 72148-72158 (2023).
6. A.J. Alazemi, and F.H. Almesri. Analysis and Simulation of a Wideband Dual-Band Balanced-to-Unbalanced Gysel Power Divider Using Coupled Lines. *Journal of Engineering Research* 11(1A): 170-183 (2023).
7. Y. Kim. Analysis method for a multi-section rat-race hybrid coupler using microstrip lines. *Journal of Electromagnetic Engineering and Science* 22(2): 95-102 (2022).
8. C. Herrojo, P. Velez, J. Munoz-Enano, L. Su, P. Casacuberta, M.G. Barba, and F. Martin. Highly sensitive defect detectors and comparators exploiting port imbalance in rat-race couplers loaded with step-impedance open-ended transmission lines. *IEEE Sensors Journal* 21(23): 26731-26745 (2021).
9. M.G.E. Kalpanadevi, M.K.N. Nishaw, E. Priyamalli, V. Radhika, and V.S. Priyanga. Design and analysis

of Wilkinson power divider using microstrip line and coupled line techniques. *IOSR Journal of Electronics and Communication Engineering (IOSR-JECE)* 34: 34-40 (2017).

10. D. Wang, X. Guo, and W. Wu. Wideband unequal power divider with enhanced power dividing ratio, fully matching bandwidth, and filtering performance. *IEEE Transactions on Microwave Theory and Techniques* 70(6): 3200-3212 (2022).
11. S. Shelar, and N. Kolhare. Design and Analysis of Hybrid Coupler. *International Journal of Engineering Research & Technology (IJERT)* 3(5): 1217-1220 (2014).
12. S. Y. Zheng, N. Kolhare, A. Gupta, Y.N. Jadhav, and H.G. Prabhakar. Design of broadband hybrid coupler with tight coupling using jumping gene evolutionary algorithm. *IEEE Transactions on Industrial Electronics* 56(8): 2987-2991 (2009).
13. N. Zhang, X. Wang, L. Zhu, and G. Lu. A novel unequal power divider with general isolation topology: Design and verification. *IEEE Microwave and Wireless Technology Letters* 33(1): 19-22 (2022).
14. M. Hayati, M.A. Sattari, S. Zarghami, and S.M. Shah-ebrahimi. Designing ultra-small Wilkinson power divider with multi-harmonics suppression. *Journal of Electromagnetic Waves and Applications* 37(4): 575-591 (2023).
15. C. Qingquan, Z. Yujin, and C. Yong. Miniaturized Wilkinson Power Divider Based on Capacitive Loading and Coupled Microstrip Line. *2022 IEEE International Conference on Microwave and Millimeter Wave Technology (ICMMT) Harbin, China* pp. 1-3 (2022).
16. I.A. Mocanu, N. Codreanu, and M. Pantazică. Design and analysis of hybrid couplers using lumped elements and microstrip topology. *2022 IEEE 28th International Symposium for Design and Technology in Electronic Packaging (SIITME) Bucharest, Romania* pp. 100-103 (2022).